A local model for the heat transfer process in two distinct flow regions

Maria Laura Martins-Costa and Rogério Martins Saldanha da Gama
Laboratório Nacional de Computação Científica, Rua Lauro Müller, Rio de Janeiro, Brazil

In the present work, a model for a local description of the energy transfer phenomenon in two distinct flow regions, one consisting of a Newtonian incompressible fluid and the other represented by a binary (solid–fluid) saturated mixture, is proposed. Compatability conditions at the interface (pure-fluid–mixture) for momentum and energy transfer are also proposed and discussed. A particular case is simulated by using an iterative procedure with a finite-difference approach, in which the inlet temperatures of both the fluid (in the pure-fluid region) and the fluid constituent (in the mixture region) are the only boundary conditions prescribed in the x-direction.

Representative results of centerline temperatures and temperature profiles are presented for the fluid in the pure-fluid region (the upper channel) as well as for both constituents in the mixture region (the lower channel), since thermal nonequilibrium is allowed.

Keywords: mixture theory; two regions flow; heat transfer; forced convection

Introduction

In the present study, the energy transfer process in two distinct flow regions is modeled with the help of the continuum theory of mixtures, a generalization of continuum mechanics (which is not appropriate for a local description of phenomena such as heat transfer in a flow through a porous medium). One flow region is occupied by a Newtonian incompressible fluid only (the usual continuum-mechanics balance equations are obviously recovered for a single-constituent mixture). In the other region, a porous medium is saturated by the above-mentioned fluid, and the fluid and the porous medium are treated as continuous constituents of a binary mixture, coexisting superposed, each of them occupying simultaneously the whole volume of the mixture. The fluid constituent, like the fluid, is assumed to be Newtonian and incompressible, while the porous matrix, represented by the "solid constituent," is assumed to be rigid, homogeneous, isotropic, and at rest.

Two similarly distinct flow regions are present in many relevant engineering situations, such as porous-bearing lubrication, flow of perforation mud in oil wells, and packed-bed heat exchangers (in which the porous matrix is only present in the vicinity of the hot–cold fluid interface, where the heat exchange is higher).

Most studies dealing with transport in porous media employ a local volume-averaging technique, discussed in detail by Whitaker (1969), to describe quantities such as temperature, pressure, concentration, and the velocity components. This technique allows the use of the classical continuum mechanics approach.

Vafai and Kim (1990) have used this approach and Darcy's law—with the addition of empirically determined terms (Brinkmann and Forchheimer extensions) to account for inertia and viscous effects and to satisfy the no-slip condition—as the balance of linear momentum. They analyzed convective flow and heat transfer in two distinct flow regions (fluid and a fluid-saturated porous medium), aiming at a fundamental investigation of the interaction phenomena at the interface, where the continuity of velocities, pressure, deviatoric normal and shear stresses, temperature, and heat flux were imposed. Assuming steady-state flow and local thermal equilibrium, they simulated a problem by means of a control volume method, studying the effects of Darcy and Prandtl numbers, of an inertia parameter (related to the Forchheimer term), and of a conductivity ratio that relates the porous-medium effective conductivity to the fluid conductivity.

Huang and Vafai (1993) have studied forced convection over a complex geometry consisting of multiple porous blocks attached to an impermeable wall. Two distinct flow regions are considered in this arrangement, which was used for flow and heat transfer control: the fluid and the fluid flowing through the porous blocks. A numerical investigation of the flow field and thermal characteristics, using a control volume method, was performed.

Thermal nonequilibrium, which comes naturally when a mixture-theory approach is employed, could also have been considered in a continuum-mechanics approach associated with a local volume-averaging technique. Such an approach was employed by Vafai and Sozen (1990), who also used Erguns' correlation as the vapor-phase momentum equation, in order to analyze the forced convective flow of a gas through a packed bed of solid particles. They concluded that, in this case, local thermal equilibrium should not be considered for high values of Reynolds number (based on the diameter of the solid particles) or Darcy number. These two numbers have a much stronger influence on the validity of the local thermal-equilibrium hypothesis than the thermophysical properties.

The use of mixture theory gives rise to new parameters (which are absent in a classical approach) in order to take into account the thermomechanical interaction among the constituents. On the other hand, mixture theory allows a local description of the flow and heat transfer processes in a porous medium, supported by a thermodynamically consistent theory,

Address reprint requests to Dr. Martins-Costa at Laboratório Nacional de Computação Científica, Rua Lauro Müller, 455-22290, Rio de Janeiro, Brazil.

Received 11 December 1993; accepted 22 July 1994

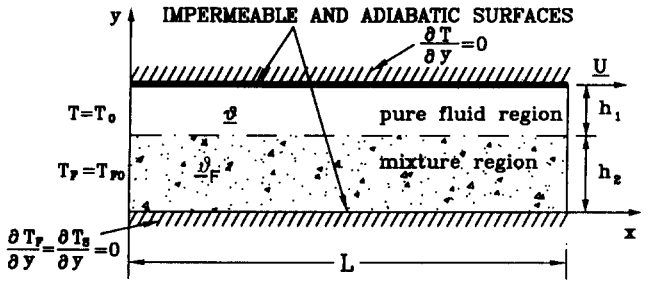

Figure 1 Problem scheme

which generalizes the classical continuum mechanics. Since both constituents are continuous, there exists simultaneously, at each spatial point, two temperatures and two velocities. The existence of two temperatures at a single point gives rise to an "energy-generation function" (which provides the thermal interaction) and the existence of two velocities gives rise to a "momentum-generation function" (which provides the dynamical interaction). Constitutive relationships for these generation functions, satisfying the Second Law of Thermodynamics, are used (Martins-Costa et al. 1992; Costa Mattos et al. 1993).

To simulate the local energy transfer phenomenon in a two-region flow problem consisting of a pure-fluid region and a binary (solid–fluid) saturated mixture region, an algorithm developed by Martins-Costa et al. (1991) is employed. An iterative procedure, based on a finite-difference approach, is used to simulate the heat transfer process in a two-region flow between two parallel insulated plates, where the fluid inlet temperature (in the pure-fluid region) and the fluid-constituent inlet temperature (in the mixture region) are the only boundary conditions prescribed in the x-direction.

Despite its simplicity, the procedure used is an effective way to perform a local simulation of the forced-convection heat transfer process that occurs when a fluid flows through two distinct regions: a pure-fluid region and a porous contiguous channel considering only realistic boundary conditions. Starting from known velocity fields (under certain conditions, these can be analytically determined), the forced-convection heating of a fluid flowing through the mentioned pure-fluid channel and porous contiguous channel in a two-dimensional (2-D) geometry (as shown in Figure 1) would give rise to a system of three second-order partial differential equations on both x- and y-variables. The structure of the energy equations allows this system to be solved with only two boundary conditions in the x-direction (one for each channel) and three in the y-direction, as well as the compatibility conditions at the interface of the pure fluid and the mixture.

From a mathematical viewpoint, this statement may sound absurd. However, from a physical viewpoint, if the pure-fluid temperature or heat flux is prescribed at the superior boundary and the temperatures or heat fluxes of both constituents are prescribed at the inferior boundaries, (y-direction), and if the inlet temperatures of the fluid (in the superior channel) and the fluid constituent (in the inferior channel) are known, no additional boundary condition is required to determine the temperature fields of the fluid and both constituents.

The procedure used in this study provides a solution for a system of three second-order partial differential equations, in two variables each, employing only five boundary conditions—three in the y-direction and only two in the x-direction—as well as the compatibility conditions at the

Notation

c Specific heat, J/kg.K
$\mathbf{D}$ Symmetrical part of the velocity gradient, 1/s
$\mathbf{D}_F$ Symmetrical part of the fluid-constituent velocity gradient, 1/s
Da Darcy number
$\mathbf{g}$ Specific gravity, m/s^2
$\mathbf{g}_i$ Specific gravity associated with the ith constituent, m/s^2
h_1 Upper-channel height, m
h_2 Lower-channel height, m
H Dimensionless height
k_F Fluid thermal conductivity, W/m.K
k_S Solid thermal conductivity, W/m.K
K Specific permeability, m^2
L Channel length, m
$\mathbf{m}_i$ Interaction force acting on the ith constituent, N/m^3
$\mathbf{n}$ Unit outward normal
p Pressure, N/m^2
$\mathbf{q}$ Heat flux, W/m^2
$\mathbf{q}_i$ ith-constituent partial heat flux, W/m^2
q''' Heat supply, W/m^3
q_i''' Heat supply to the ith-constituent, W/m^3
R Internal heat-supply factor, W/m^3.K
$\mathbf{t}$ Tangent vector
T Temperature, K
T_i ith-constituent temperature, K
$\mathbf{U}$ Moving plate velocity, m/s
$\mathbf{v}$ Fluid velocity (vector field), m/s
v x-component of fluid velocity, m/s
$\mathbf{v}_F$ Fluid-constituent velocity (vector field), m/s
v_F x-component of fluid-constituent velocity, m/s
$\bar{v}$ Average velocity for the pure-fluid region, m/s
v^* Dimensionless velocity relating pressure drop to moving plate velocity
X Dimensionless x-variable
Y Dimensionless y-variable

Greek symbols

α Dimensionless velocity
α_F Fluid constituent dimensionless velocity
β Dimensionless thermal conductivity
β_i ith-constituent dimensionless thermal conductivity
γ Aspect ratio
ε Dimensionless internal heat supply factor
η Fluid viscosity, kg/m.s
θ Dimensionless temperature
θ_i ith-constituent dimensionless temperature
λ Parameter depending on porous matrix
Λ Parameter related to mixture structure
ρ Fluid density (as a continuum), kg/m^3
ρ_i ith-constituent density, kg/m^3
φ Porosity
$\boldsymbol{\sigma}$ Stress tensor, N/m^2
$\boldsymbol{\sigma}_i$ ith-constituent partial stress tensor, N/m^2
ψ_i ith-constituent internal heat supply, W/m^3
Ω_1 Open set representing pure fluid region
Ω_2 Open set representing mixture region

Subscripts

F Fluid constituent
i ith-constituent
S Solid constituent

interface of the pure fluid and the mixture. In fact, an exhaustive number of examples taken into consideration have shown that the temperatures inside both channels are not affected by additional boundary conditions in the x-direction, which can even lead to unrealistic situations on the boundaries.

Mathematical model

If we represent the region occupied by the pure fluid by the open set Ω_1, with boundary $\partial\Omega_1$, and if we represent the region occupied by the mixture by the open set Ω_2, with boundary $\partial\Omega_2$, then the mass balance for the considered phenomenon may be written as

$$\frac{\partial \rho}{\partial t} + \operatorname{div}(\rho \mathbf{v}) = 0 \quad \text{in} \quad \Omega_1 \tag{1}$$

$$\frac{\partial \rho_i}{\partial t} + \operatorname{div}(\rho_i \mathbf{v}_i) = 0 \quad \text{in} \quad \Omega_2,\ i = 1, n \tag{2}$$

in which n is the number of constituents in the mixture region, ρ is the actual fluid density in Ω_1, $\mathbf{v}$ is the fluid velocity in Ω_1, ρ_i is the ith constituent mass density in Ω_2, and $\mathbf{v}_i$ is the ith constituent velocity in Ω_2. The field ρ_i is locally defined as the ratio between the ith constituent mass and the respective volume of the mixture.

Since the mass of each constituent is preserved, the mass of the mixture as a whole is automatically conserved.

The balance of linear momentum is given by

$$\rho\left[\frac{\partial \mathbf{v}}{\partial t} + (\operatorname{grad} \mathbf{v})\mathbf{v}\right] = \operatorname{div} \boldsymbol{\sigma} + \rho \mathbf{g} \quad \text{in} \quad \Omega_1 \tag{3}$$

$$\rho_i\left[\frac{\partial \mathbf{v}_i}{\partial t} + (\operatorname{grad} \mathbf{v}_i)\mathbf{v}_i\right] = \operatorname{div} \boldsymbol{\sigma}_i + \mathbf{m}_i + \rho_i \mathbf{g}_i \quad \text{in} \quad \Omega_2,\ i = 1, n \tag{4}$$

in which $\boldsymbol{\sigma}$ is the Cauchy stress tensor, $\boldsymbol{\sigma}_i$ is the partial stress tensor associated with the ith constituent, $\mathbf{g}$ is a body force per unit mass, $\mathbf{g}_i$ is a body force per unit mass acting on the ith constituent, and $\mathbf{m}_i$ is an interaction force per unit volume acting on the ith constituent due to its interaction with the other constituents of the mixture.

The momentum source $\mathbf{m}_i$ arises from the existence of more than one velocity at each point in the mixture region. Since $\mathbf{m}_i$ is an internal contribution, the following must hold everywhere:

$$\sum_{i=1}^{n} \mathbf{m}_i = 0 \quad \text{in} \quad \Omega_2 \tag{5}$$

In the present study, the partial stress tensor is assumed to be symmetrical as the Cauchy stress tensor, satisfying automatically the angular momentum balance.

The energy balance is given by

$$\rho c\left[\frac{\partial T}{\partial t} + (\operatorname{grad} T)\cdot \mathbf{v}\right] = -\operatorname{div} \mathbf{q} + q''' + \boldsymbol{\sigma}\cdot\mathbf{D} \quad \text{in} \quad \Omega_1 \tag{6}$$

$$\rho_i c_i\left[\frac{\partial T_i}{\partial t} + (\operatorname{grad} T_i)\cdot \mathbf{v}_i\right] = -\operatorname{div} \mathbf{q}_i + q_i''' + \psi_i + \boldsymbol{\sigma}_i\cdot\mathbf{D}_i \quad \text{in} \quad \Omega_2,\ i = 1, n \tag{7}$$

in which T is the fluid temperature in Ω_1, T_i is the ith constituent temperature in Ω_2, c is the fluid specific heat, c_i the ith constituent specific heat, $\mathbf{D}$ is the symmetrical part of the velocity gradient in Ω_1, $\mathbf{D}_i$ is the symmetrical part of the ith constituent velocity gradient, $\mathbf{q}$ is the heat flux (per unit time and unit area) in Ω_1, $\mathbf{q}_i$ is the partial heat flux (per unit time and unit area) associated with the ith constituent in Ω_2, q''' is an external heat supply (per unit time and unit volume), q_i''' is the external heat supply (per unit time and unit volume) to the ith constituent, and ψ_i is an internal heat supply.

The field ψ_i represents the amount of energy, per unit time and unit volume, supplied to the ith constituent, arising from its thermal interaction with the remaining constituents of the mixture. Since ψ_i is an internal contribution, the following must hold everywhere (Martins-Costa et al. 1992, 1993):

$$\sum_{i=1}^{n} \psi_i = 0 \quad \text{in} \quad \Omega_2 \tag{8}$$

In this study, the region Ω_2 is occupied by a binary mixture (saturated porous medium) whose constituents are a Newtonian incompressible fluid and a rigid, isotropic, and homogeneous porous matrix at rest, with a porosity φ.

Since the porous matrix is at rest, the continuity and momentum equations for the solid constituent (which represents the porous medium in the mixture) will not be solved.

In addition, since the fluid is Newtonian (in $\Omega_1 \cup \Omega_2$), the following constitutive equations are employed (Williams 1978):

$$\boldsymbol{\sigma} = -p\mathbf{1} + 2\eta\mathbf{D} \quad \text{in} \quad \Omega_1 \tag{9}$$

$$\boldsymbol{\sigma}_F = -\varphi p\mathbf{1} + 2\lambda\varphi^2\eta\mathbf{D}_F \quad \text{in} \quad \Omega_2 \tag{10}$$

$$\mathbf{m}_F = -\frac{\varphi^2\eta}{K}\mathbf{v}_F \quad \text{in} \quad \Omega_2 \tag{11}$$

where η is the actual fluid viscosity, K is the specific permeability, λ is a scalar parameter depending on the porous matrix microstructure, and the index F refers to the fluid constituent.

The heat flux in Ω_1, the partial heat flux in Ω_2, and the internal supplies ψ_F and ψ_S (the latter referring to the solid constituent) are given by Martins-Costa et al. (1992) and Costa Mattos et al. (1993):

$$\mathbf{q} = -k_F \operatorname{grad} T \quad \text{in} \quad \Omega_1 \tag{12}$$

$$\mathbf{q}_F = -\Lambda k_F\, \varphi \operatorname{grad} T_F \quad \text{in} \quad \Omega_2 \tag{13}$$

$$\mathbf{q}_S = -\Lambda k_S(1-\varphi) \operatorname{grad} T_S \quad \text{in} \quad \Omega_2 \tag{14}$$

$$\psi_F = -\psi_S = R(T_S - T_F) \quad \text{in} \quad \Omega_2 \tag{15}$$

in which k_F is the Newtonian fluid thermal conductivity and K_S is the porous matrix thermal conductivity. In Equations 13 and 14, Λ represents a scalar positive-valued parameter that may depend on both the internal structure and the kinematics of the mixture. In Equation 15, R is a positive-valued factor that depends not only on spatial position and on both constituents' thermal properties but also on the velocity of both constituents, accounting for the convective heat transfer. Since the solid constituent is supposed to be at rest, only the velocity of the fluid constituent would influence the factor R, but this influence will be neglected in the present study.

The interface between the regions Ω_1 and Ω_2 is defined by the set $\partial\Omega_I \equiv \bar{\Omega}_1 \cap \bar{\Omega}_2$. At this interface, some compatibility conditions must be imposed in order to allow the solution of the problem. According to Williams (1978), since there is no flow across the interface, the following relations must hold:

$$\mathbf{v} = \varphi\mathbf{v}_F \tag{16}$$

$$\varphi\boldsymbol{\sigma}\mathbf{n}\cdot\mathbf{t} = \boldsymbol{\sigma}_F\mathbf{n}\cdot\mathbf{t} \tag{17}$$

in which $\mathbf{n}$ is an outward normal to $\partial\Omega_I$ and $\mathbf{t}$ is any tangent to $\partial\Omega_I$. The compatibility equations (Equations 16 and 17) simulate the experimental condition proposed by Beavers and Joseph (1967), which was confirmed and generalized by several

authors (see, e.g., Nield and Bejan 1992). The idealized model for a porous medium, employed by Taylor (1971) and Richardson (1971), gives theoretical support to Beavers and Joseph's condition. Equations 16 and 17, obtained from the solution of thermodynamically consistent equations (derived by means of a mixture-theory viewpoint) in both regions, do not suffer from the difficulty of matching the porous-medium flow equations with the Navier–Stokes equation, discussed by Nield and Bejan (1992). Williams (1978), based on a no-slip condition, concluded that the velocity should be zero on the solid parts of the boundary (since the porous matrix is at rest) and should match the fluid-diffusing velocity on the fluid parts of the boundary. He also supposed that both solid and fluid receive shearing stress from the fluid stream at the pure-fluid region. It should be noticed that, at the interface, the pure-fluid velocity is distinct from the fluid-constituent velocity (in the mixture region) when a mixture-theory viewpoint is considered.

To assure that the temperature field is continuous and that the normal heat flux is both continuous and adequately distributed throughout the interface, the following compatibility conditions are imposed at the interface $\partial\Omega_I$:

$$T = \varphi T_F + (1-\varphi) T_S \quad \text{at} \quad \partial\Omega_I \tag{18}$$

$$\varphi \mathbf{q}\cdot\mathbf{n} = q_F \cdot \mathbf{n} \quad \text{at} \quad \partial\Omega_I \tag{19}$$

$$(1-\varphi)\mathbf{q}\cdot\mathbf{n} = \mathbf{q}_S \cdot \mathbf{n} \quad \text{at} \quad \partial\Omega_I \tag{20}$$

where Equation 18 represents the continuity in the temperature field (the temperature of the fluid must be equal to the temperature of the mixture at the interface), while Equations 19 and 20 represent the distribution of the heat flux from/to the mixture, at the interface.

Vafai and Kim (1990) have imposed continuity of temperature and heat-flux fields, which could be considered analogous to Equations 18 to 21, provided that thermal nonequilibrium is allowed.

Now, taking into account that

$$\Omega_1 \equiv \{(x, y) \quad \text{such that} \quad 0 < x < L,\ h_2 < y < h_1 + h_2\}$$

$$\Omega_2 \equiv \{(x, y) \quad \text{such that} \quad 0 < x < L,\ 0 < y < h_2\}$$

$$\partial\Omega_I \equiv \{(x, y) \quad \text{such that} \quad 0 < x < L,\ y = h_2\}$$

and assuming that the flow is not affected by the thermal problem, the velocity fields in Ω_1 and Ω_2 may be analytically obtained, provided that a one-dimensional (1-D) steady-state horizontal flow is assumed.

Denoting by v and v_F the x-components of $\mathbf{v}$ and $\mathbf{v}_F$, and taking into account that $\rho_F = \varphi\rho$, the hydrodynamical problem (Equations 1 to 5, 9 to 11, 16, and 17) is represented by

$$\eta \frac{d^2 v}{dy^2} - \frac{\partial p}{\partial x} = 0 \quad 0 < x < L,\ h_2 < y < h_1 + h_2 \tag{21}$$

$$\lambda\varphi^2\eta \frac{d^2 v_F}{dy^2} - \varphi \frac{\partial p}{\partial x} - \frac{\varphi^2\eta}{K} v_F = 0 \quad 0 < x < L,\ 0 < y < h_2 \tag{22}$$

$$v = U \qquad 0 < x < L,\ y = h_1 + h_2 \tag{23}$$

$$v_F = 0 \qquad 0 < x < L,\ y = 0 \tag{24}$$

$$v = \varphi v_F \qquad 0 < x < L,\ y = h_2 \tag{25}$$

$$\frac{dv}{dy} = \lambda\varphi \frac{dv_F}{dy} \qquad 0 < x < L,\ y = h_2 \tag{26}$$

The solution of Equations 21 to 26, given by Saldanha da Gama and Sampaio (1983)

$$v = U\left[\frac{\sqrt{\frac{K}{\lambda}}\,\mathrm{tgh}\left(\frac{h_2}{\sqrt{K\lambda}}\right) + y - h_2}{\sqrt{\frac{K}{\lambda}}\,\mathrm{tgh}\left(\frac{h_2}{\sqrt{K\lambda}}\right) + h_1}\right] - \frac{1}{2\eta}\frac{\partial p}{\partial x}\left[(h_1+h_2)^2 - y^2\right] + \frac{1}{2\eta}\frac{\partial p}{\partial x}(y - h_1 - h_2)$$
$$\times\left[\frac{2\left(\frac{\cosh\left(\frac{h_2}{\sqrt{K\lambda}}\right) - 1}{\cosh\left(\frac{h_2}{\sqrt{K\lambda}}\right)}\right)\frac{K}{h_1} - 2h_2 - h_1 - \frac{2h_2}{h_1}\sqrt{\frac{K}{\lambda}}\,\mathrm{tgh}\left(\frac{h_2}{\sqrt{K\lambda}}\right)}{1 + \frac{1}{h_1}\sqrt{\frac{K}{\lambda}}\,\mathrm{tgh}\left(\frac{h_2}{\sqrt{K\lambda}}\right)}\right] \tag{27}$$

for $h_2 < y < h_1 + h_2$ (the pure-fluid region), is the fluid velocity, and the corresponding solution

$$v_F = U\left[\frac{\frac{1}{\varphi}\sqrt{\frac{K}{\lambda}}\sinh\left(\frac{y}{\sqrt{K\lambda}}\right)}{\left(\sqrt{\frac{K}{\lambda}}\,\mathrm{tgh}\left(\frac{h_2}{\sqrt{K\lambda}}\right) + h_1\right)\cosh\left(\frac{h_2}{\sqrt{K\lambda}}\right)}\right] + \frac{K}{\eta\varphi}\frac{\partial p}{\partial x}\left[\cosh\left(\frac{y}{\sqrt{K\lambda}}\right) - 1\right] - \frac{K}{\eta\varphi}\frac{\partial p}{\partial x}\sinh\left(\frac{y}{\sqrt{K\lambda}}\right)$$
$$\times\left[\frac{\sqrt{\frac{K}{\lambda}}\left(\frac{\cosh\left(\frac{h_2}{\sqrt{K\lambda}}\right) - 1}{h_1\cosh\left(\frac{h_2}{\sqrt{K\lambda}}\right)}\right) + \mathrm{tgh}\left(\frac{h_2}{\sqrt{K\lambda}}\right) + \frac{h_1}{2\sqrt{K\lambda}\cosh\left(\frac{h_2}{\sqrt{K\lambda}}\right)}}{1 + \frac{1}{h_1}\sqrt{\frac{K}{\lambda}}\,\mathrm{tgh}\left(\frac{h_2}{\sqrt{K\lambda}}\right)}\right] \tag{28}$$

for $0 < y < h_2$ (the mixture region), is the fluid-constituent velocity.

Assuming q''' and q_i''' equal to zero and neglecting $\boldsymbol{\sigma}\cdot\mathbf{D}$ and $\boldsymbol{\sigma}_F\cdot\mathbf{D}_F$, the energy equations (Equations 6 to 8, 12 to 15, and 18 to 22) reduce to

$$\rho c_F v \frac{\partial T}{\partial x} = k_F \left[\frac{\partial^2 T}{\partial x^2} + \frac{\partial^2 T}{\partial y^2}\right] \qquad 0 < x < L,\ h_2 < y < h_1 + h_2 \tag{29}$$

$$\varphi \rho c_F v_F \frac{\partial T_F}{\partial x} = \Lambda k_F \varphi \left[\frac{\partial^2 T_F}{\partial x^2} + \frac{\partial^2 T_F}{\partial y^2}\right] + R(T_s - T_F) \qquad 0 < x < L,\ 0 < y < h_2 \tag{30}$$

$$0 = \Lambda k_s (1-\varphi)\left[\frac{\partial^2 T_S}{\partial x^2} + \frac{\partial^2 T_S}{\partial y^2}\right] + R(T_F - T_S) \qquad 0 < x < L,\ 0 < y < h_2 \tag{31}$$

subject to the boundary conditions

$$T = T_0 \qquad x = 0,\ h_2 < y < h_1 + h_2 \tag{32}$$

$$T_F = T_{F0} \qquad x = 0,\ 0 < y < h_2 \tag{33}$$

$$\frac{\partial T}{\partial y} = 0 \qquad 0 < x < L,\ y = h_1 + h_2 \tag{34}$$

$$\frac{\partial T_F}{\partial y} = 0 \qquad 0 < x < L,\ y = 0 \tag{35}$$

$$\frac{\partial T_S}{\partial y} = 0 \qquad 0 < x < L,\ y = 0 \tag{36}$$

and to the compatibility conditions at the interface:

$$T = \varphi T_F + (1-\varphi) T_S \qquad 0 < x < L,\ y = h_2 \tag{37}$$

$$\frac{\partial T}{\partial y} = \Lambda \frac{\partial T_F}{\partial y} \qquad 0 < x < L,\ y = h_2 \tag{38}$$

$$\frac{\partial T}{\partial y} = \Lambda \frac{k_S}{k_F} \frac{\partial T_S}{\partial y} \qquad 0 < x < L,\ y = h_2 \tag{39}$$

The problem is put in a dimensionless form by using the following dimensionless variables:

$$X = \frac{x}{L} \qquad Y = \frac{y}{h_1 + h_2} \tag{40}$$

$$\theta = \frac{T}{T_0} \quad \theta_F = \frac{T_F}{T_0} \qquad \theta_S = \frac{T_S}{T_0} \tag{41}$$

$$\alpha = \frac{v}{\bar{v}} \qquad \alpha_F = \frac{v_F}{\bar{v}} \tag{42}$$

$$\beta = \frac{k_F}{\rho c_F L \bar{v}} \qquad \beta_F = \frac{k_F \Lambda}{\rho c_F L \bar{v}} \qquad \beta_S = \frac{k_S}{\rho c_F L \bar{v}} \frac{1-\varphi}{\varphi} \tag{43}$$

$$\gamma = \frac{L}{h_1 + h_2} \qquad \varepsilon = \frac{RL}{\rho c_F \bar{v} \varphi} \qquad H = \frac{h_2}{h_1 + h_2} \tag{44}$$

where $\bar{v}$, which represents an average velocity for the pure-fluid region, considering $K = 0$ and $\varphi = 0$ in the porous medium, is defined as

$$\bar{v} = \frac{1}{2} U - \frac{1}{12\eta} \frac{\partial p}{\partial x} h_1^2 \tag{45}$$

Equations 29 to 31 yields

$$\alpha \frac{\partial \theta}{\partial X} = \beta \left[\frac{\partial^2 \theta}{\partial X^2} + \gamma \frac{\partial^2 \theta}{\partial Y^2}\right] \tag{46}$$

$$\alpha_F \frac{\partial \theta_F}{\partial X} = \beta_F \left[\frac{\partial^2 \theta_F}{\partial X^2} + \gamma \frac{\partial^2 \theta_F}{\partial Y^2}\right] + \varepsilon(\theta_S - \theta_F) \tag{47}$$

$$0 = \beta_S \left[\frac{\partial^2 \theta_S}{\partial X^2} + \gamma \frac{\partial^2 \theta_S}{\partial Y^2}\right] + \varepsilon(\theta_F - \theta_S) \tag{48}$$

where Equation 46 is valid for $H < Y < 1$, representing the pure fluid in the upper channel, and Equations 47 and 48 are valid for $0 < Y < H$, representing both constituents in the lower channel. The problem is subject to the following boundary conditions:

$$\theta(0, Y) = \theta_0 \quad \text{for} \quad H < Y < 1 \tag{49}$$

$$\theta_F(0, Y) = \theta_{F0} \quad \text{for} \quad 0 < Y < H \tag{50}$$

$$\frac{\partial \theta}{\partial Y}(X, 1) = 0 \qquad \frac{\partial \theta_F}{\partial Y}(X, 0) = 0 \qquad \frac{\partial \theta_S}{\partial Y}(X, 0) = 0 \qquad \text{for } 0 < X < 1 \tag{51}$$

and the following compatibility conditions are verified at the interface:

$$\theta(X, H) = \varphi \theta_F(X, H) + (1-\varphi)\theta_S(X, H) \quad \text{for} \quad 0 < X < 1 \tag{52}$$

$$\frac{\partial \theta}{\partial Y}(X, H) = \Lambda \frac{\partial \theta_F}{\partial Y}(X, H) \quad \text{for} \quad 0 < X < 1 \tag{53}$$

$$\frac{\partial \theta}{\partial Y}(X, H) = \Lambda \frac{k_S}{k_F} \frac{\partial \theta_S}{\partial Y}(X, H) \quad \text{for} \quad 0 < X < 1 \tag{54}$$

Numerical method

The heat transfer problem (Equations 46 to 54) consists of a system of three second-order differential equations, on both X- and Y-variables, subject to three boundary conditions in the Y-direction, two boundary conditions in the X-direction, and three compatibility conditions at the interface that relate the fluid temperature to the temperatures of both constituents. It should be noticed that the solid-constituent inlet ($\theta_S(0, Y)$) and outlet ($\theta_S(1, Y)$) dimensionless temperatures, as well as the fluid outlet ($\theta(1, Y)$) and the fluid-constituent outlet ($\theta_F(1, Y)$) dimensionless temperatures, are not prescribed.

From a mathematical viewpoint, a problem of this kind (Equations 46 to 54) consisting of three elliptic equations, on both X- and Y-variables, even if physically realistic, could give rise to an infinite number of solutions (John 1982). However, a great number of tested situations have shown that additional boundary conditions in the x-direction have no influence on both solid- and fluid-constituent bulk temperatures in the mixture region or on the fluid bulk temperature in the pure fluid region.

An iterative procedure is used, so that three second-order equations on the x-variable (Equations 46 to 48) can be solved with the help of two boundary conditions in the x-direction, one for each considered region: the fluid inlet temperature in the pure-fluid region (Equation 49) and the fluid-constituent inlet temperature in the mixture region (Equation 50). The problem is treated as a sequence of modified problems in which the second-order derivatives on the x-direction, for the fluid and both constituents, are treated as previously known fields; that is, energy equations of the fluid (Equation 46) and of the fluid constituent (Equation 47) are treated as a sequence of

parabolic problems on the X-variable, while the solid-constituent energy equation (Equation 48) can be considered as a sequence of ordinary problems on the Y-variable. The original system of equations is modified to

$$\left[\frac{\alpha}{\beta}\frac{\partial\theta}{\partial X} - \gamma\frac{\partial^2\theta}{\partial Y^2}\right]^l = \left[\frac{\partial^2\theta}{\partial X^2}\right]^{l-1} \tag{55}$$

$$\left[\frac{\alpha_F}{\beta_F}\frac{\partial\theta_F}{\partial X} - \gamma\frac{\partial^2\theta_F}{\partial Y^2} - \frac{\varepsilon}{\beta_F}(\theta_S - \theta_F)\right]^l = \left[\frac{\partial^2\theta_F}{\partial X^2}\right]^{l-1} \tag{56}$$

$$\left[-\gamma\frac{\partial^2\theta_S}{\partial Y^2} - \frac{\varepsilon}{\beta_S}(\theta_F - \theta_S)\right]^l = \left[\frac{\partial^2\theta_S}{\partial X^2}\right]^{l-1} \tag{57}$$

where the derivatives $\partial^2\theta/\partial X^2$, $\partial^2\theta_F/\partial X^2$, and $\partial^2\theta_S/\partial X^2$ are calculated from a previous iteration.

Since no analytical solution to the system of Equations 55 to 57 is known, numerical approximations to its solution are sought with the help of a finite-difference approach (Euvrard 1987). For the diffusive terms, a central finite-difference-scheme discretization was used, while an "upwind" scheme was employed in the convective-term discretization.

Since the temperature-coefficients matrix (associated with the modified system of Equations 55 to 57) is sparse, a grid description, in which each constituent temperature possesses two indexes according to its position on the grid, is used. Each iteration l, represented in such a way as to allow an effective storage scheme with memory reutilization, is then solved with the help of the Gauss–Seidel method. The approximations for the second-order derivatives of the fluid and both constituents are calculated from a previous $(l-1)$ iteration by means of a central finite-difference scheme.

The procedure can be summarized in the following way: to start the scheme, initial values are estimated for the second-order derivatives with respect to X. This allows us to solve Equations 55 to 57 in order to obtain the dimensionless temperature fields: θ, θ_F, and θ_S. These are stored and subsequently used to calculate new approximations for $\partial^2\theta/\partial X^2$, $\partial^2\theta_F/\partial X^2$, and $\partial^2\theta_S/\partial X^2$. These approximations are then employed in the next step to calculate new values for θ, θ_F, and θ_S. These vectors are compared to the ones previously stored, and the process is carried on until convergence is achieved.

Vafai and Kim (1990) have used a different procedure in order to disconsider upstream conditions: they employed a much longer computational domain, which enabled them to be sure that the conditions at the channel's outlet would not affect the bulk temperature. In the present work, on the other hand, different boundary conditions such as prescribed temperatures (for both constituents and the fluid, varying from 0 to 1) and prescribed heat fluxes were employed at the outlet. It was verified that all those tested boundary conditions cause no alteration on the temperature profiles except for the last nodes in the X-direction.

The control volume method has already been successfully applied to problems arising from a mixture-theory approach when the hydrodynamical and thermal problems were coupled (Martins-Costa et al. 1994).

Results

Figure 2 shows the dimensionless velocity profiles for the pure fluid (α, in the pure-fluid region) and for the fluid constituent (α_F, in the mixture region). The variation of α_F can only be observed in a detail with a modified scale, as shown in the lower portion of the figure.

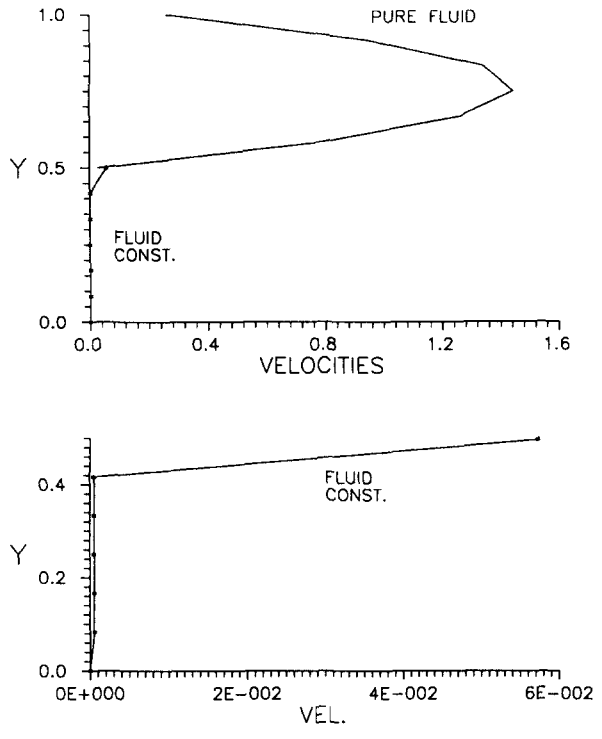

Figure 2 Dimensionless velocities α and α_F for $\varepsilon = 2.64 \times 10^{-3}$, $\gamma = 30$, $H = 1/2$, $\mathrm{Da} = 2.5 \times 10^{-5}$, $v^* = 20/3$

Centerline dimensionless temperatures (for each channel) versus the longitudinal coordinate X for both the pure-fluid and the mixture regions (this one with two distinct temperature profiles, one for each constituent) are presented, as well as the temperature profiles at a central section for some representative cases. Two long, adjacent channels (both of the same height) are considered; the fluid dimensionless inlet temperature (in the upper channel) is 1, and the fluid-constituent dimensionless inlet temperature (in the lower channel) is 0. A coarse grid, with seven nodes in the x-direction and 13 nodes in the y-direction, was used in the numerical approximation.

At this point, it is appropriate to define Darcy's number and a dimensionless velocity v^* that is based on the pure-fluid average velocity and that relates the effect of pressure drop to the effect of the moving plate velocity. These definitions are as follows:

$$\mathrm{Da} = \frac{K}{h_2^2} \tag{58}$$

$$v^* = -\frac{\partial p}{\partial x}\frac{h_1^2}{6\eta U} \tag{59}$$

Figures 3 to 5 show the influence of the dimensionless velocity v^* on the dimensionless temperatures of the fluid and of both constituents. Comparing Figures 3 and 4 (in which the only varying parameter is Darcy's number, which is 2.5×10^{-3} in Figure 3 and 2.5×10^{-5} in Figure 4), it can be observed that, for small values of permeability, both constituents' temperatures tend toward the fluid temperature (which suffers almost no variation along the superior channel). It is important to mention that the scale of the temperature profile in Figure 4 has been modified. Comparing Figures 4 ($v^* = 2/3$) and 5 ($v^* = 20/3$), the influence of the pressure drop may be observed, since it is ten times greater in Figure 5 than in Figure 4. In Figure 5, the temperature profiles in the central section are very distinct.

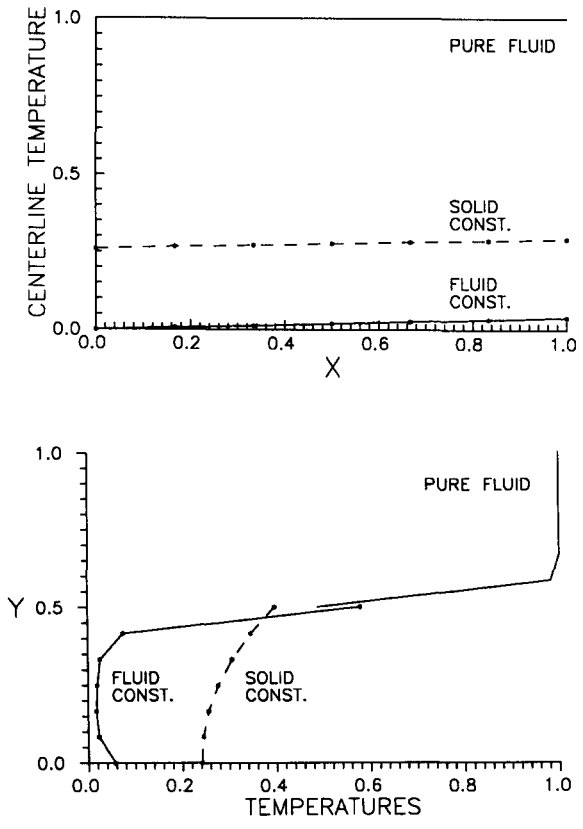

Figure 3 Centerline temperature and temperature profiles for $\varepsilon = 6.86 \times 10^{-3}$, $\gamma = 30$, $H = 1/2$, $\beta = \beta_F = 1.43 \times 10^{-7}$, $\beta_S = 1.43 \times 10^{-6}$, Da $= 2.5 \times 10^{-3}$, $v^* = 2/3$

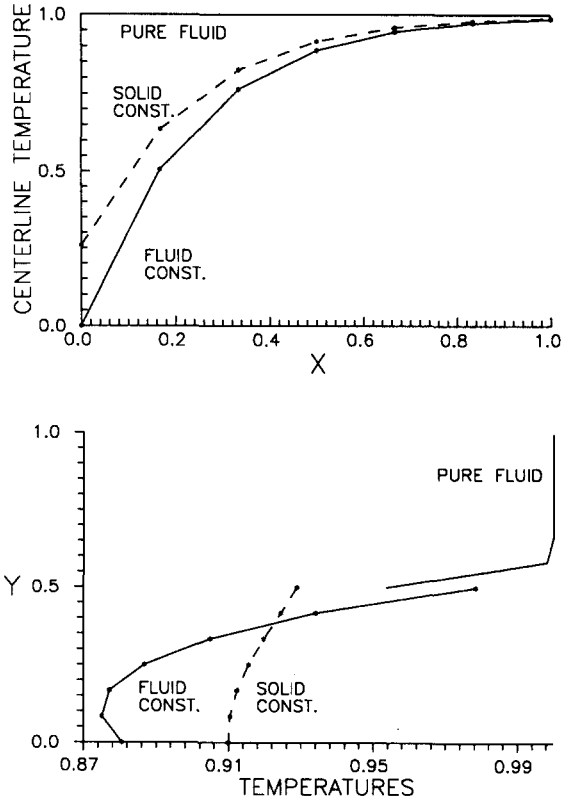

Figure 4 Centerline temperature and temperature profiles for $\varepsilon = 6.86 \times 10^{-3}$, $\gamma = 30$, $H = 1/2$, $\beta = \beta_F = 1.43 \times 10^{-7}$, $\beta_S = 1.43 \times 10^{-6}$, Da $= 2.5 \times 10^{-5}$, $v^* = 2/3$

The influence of the thermal conductivity on the temperatures may be observed by comparing Figure 5 to Figure 6, in which the fluid thermal conductivity was made ten times smaller than that used in all the remaining figures (β_F is 5.5×10^{-8} and 5.5×10^{-9}, respectively, in Figures 5 and 6).

In Figure 7, the temperature profiles in the central section and the dimensionless temperatures for each channel are plotted for $v^* = \frac{2}{30}$, which is a value ten times smaller than that used for v^* in Figure 3. The influence of the upper channel (the hot channel) is stronger for smaller velocities.

The influence of the porous matrix permeability may be observed by comparing Figure 7 to Figure 8, in which Darcy's number is made 100 times smaller. A comparison between Figures 4 and 8 shows the influence of the dimensionless velocity v^*, which is made ten times smaller in Figure 8. In both figures, modified scales are used for the central-section temperature profiles. For smaller velocities, all the temperatures tend to a common value, before the central section.

The influence of the inlet temperatures in both channels may be observed by comparing Figure 3 to Figure 9. Figure 9 was plotted for the same parameters used in Figure 3, except for the boundary conditions. The fluid inlet temperature (in the pure-fluid region) is made 0, while the fluid-constituent inlet temperature (in the mixture region) is made 1.

Final remarks

In this study, the energy transfer in two distinct flow regions is modeled, in a context of thermal nonequilibrium based on a systematic local theory: the continuum theory of mixtures. In the porous region, both fluid and solid (the porous matrix)

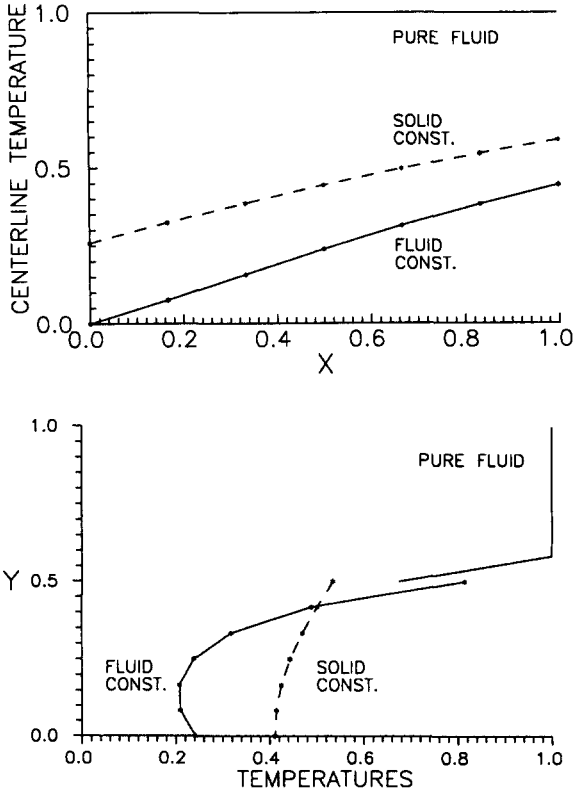

Figure 5 Centerline temperature and temperature profiles for $\varepsilon = 2.64 \times 10^{-3}$, $\gamma = 30$, $H = 1/2$, $\beta = \beta_F = 5.5 \times 10^{-8}$, $\beta_S = 5.5 \times 10^{-7}$, Da $= 2.5 \times 10^{-5}$, $v^* = 20/3$

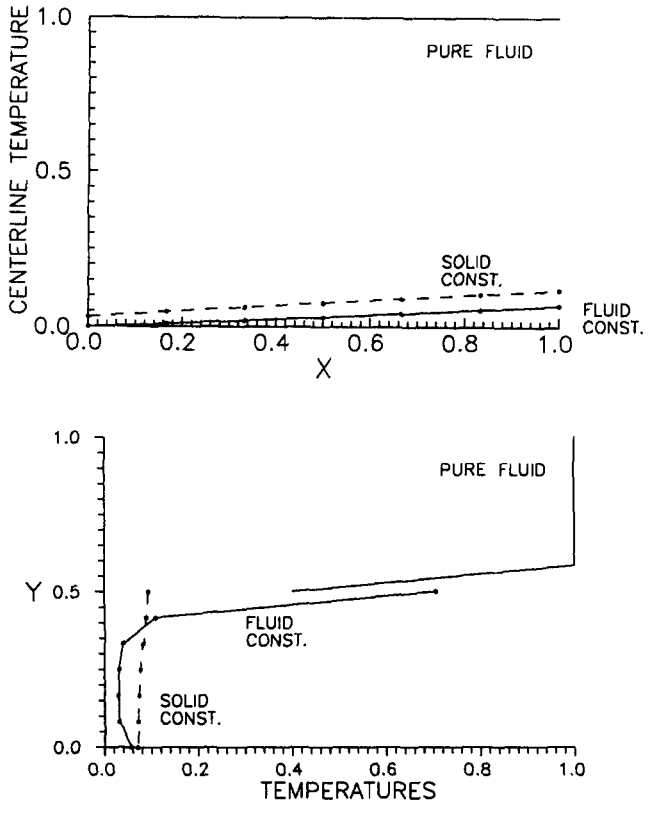

Figure 6 Centerline temperature and temperature profiles for $\varepsilon = 2.64 \times 10^{-3}$, $\gamma = 30$, $H = 1/2$, $\beta = \beta_F = 5.5 \times 10^{-9}$, $\beta_S = 5.5 \times 10^{-7}$, $Da = 2.5 \times 10^{-5}$, $v^* = 20/3$

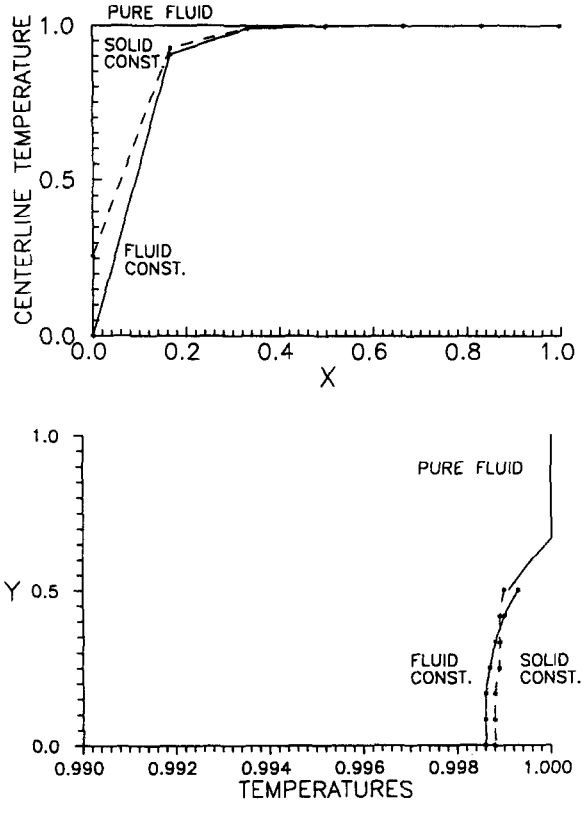

Figure 8 Centerline temperature and temperature profiles for $\varepsilon = 1.07 \times 10^{-2}$, $\gamma = 30$, $H = 1/2$, $\beta = \beta_F = 2.23 \times 10^{-7}$, $\beta_S = 2.23 \times 10^{-6}$, $Da = 2.5 \times 10^{-5}$, $v^* = 1/15$

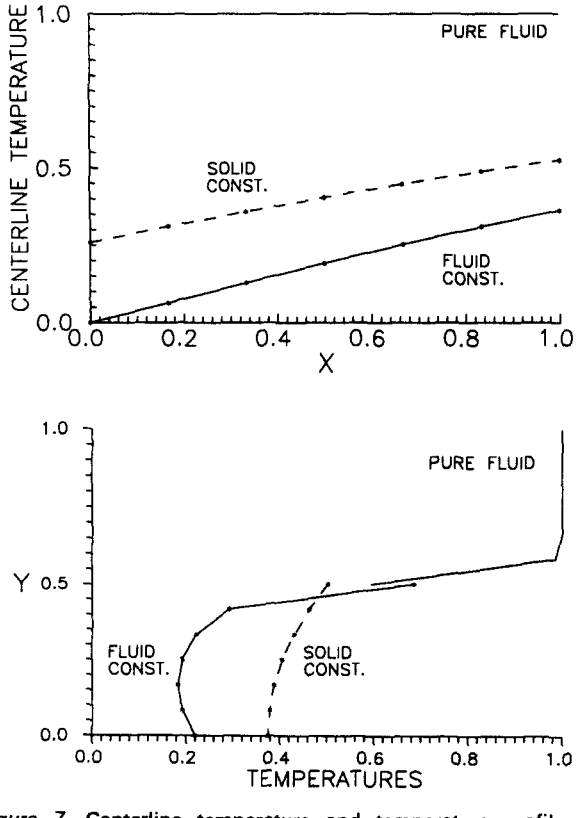

Figure 7 Centerline temperature and temperature profiles for $\varepsilon = 1.07 \times 10^{-2}$, $\gamma = 30$, $H = 1/2$, $\beta = \beta_F = 2.23 \times 10^{-7}$, $\beta_S = 2.23 \times 10^{-6}$, $Da = 2.5 \times 10^{-3}$, $v^* = 1/15$

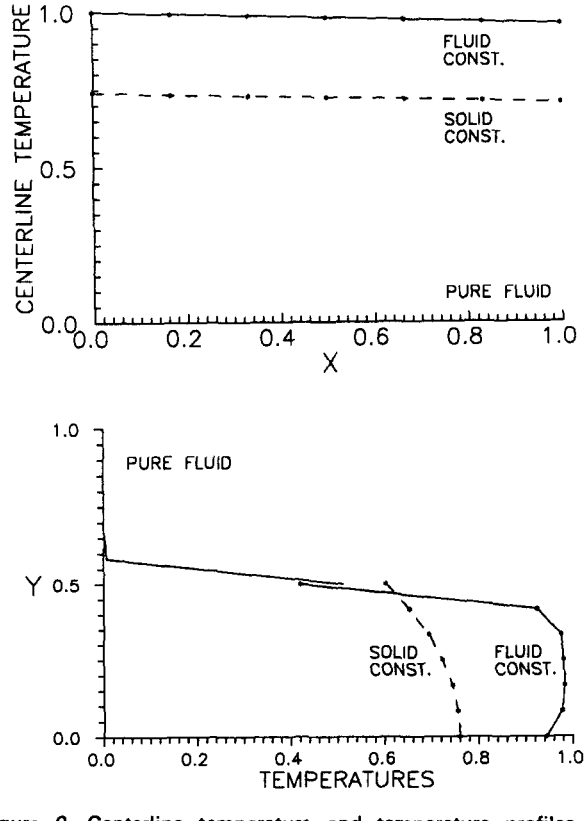

Figure 9 Centerline temperature and temperature profiles for $\varepsilon = 6.86 \times 10^{-3}$, $\gamma = 30$, $H = 1/2$, $\beta = \beta_F = 1.43 \times 10^{-7}$, $\beta_S = 1.43 \times 10^{-6}$, $Da = 2.5 \times 10^{-3}$, $v^* = 2/3$

are treated as continuous constituents of a binary mixture, and the classical (continuum mechanics) balance equations are recovered in the pure-fluid region, where the mixture is reduced to a single constituent.

Conditions at the interface between the pure fluid and the mixture were imposed in order to assure the continuity of the temperature and the heat flux, but the heat-flux decomposition was arbitrarily chosen.

An iterative procedure, in which the inlet temperatures for both the fluid and the fluid constituent are the only boundary conditions prescribed in the x-direction, simulates the problem by using available boundary information only. In fact, this procedure estimates, indirectly, the three missing boundary conditions.

Most of the studies on transport phenomena in porous media use a volume-averaging technique based on a continuum mechanics approach. A different approach is used in this study. The continuum theory of mixtures, which generalizes the classical continuum mechanics, allows the construction of a thermodynamically consistent local model by means of a systematic procedure to describe the transport phenomena in two distinct flow regions: a fluid and a fluid-saturated porous medium. The cost associated with the use of this mixture theory is not high. In fact, the only changes required are a few new definitions and some new terms in the balance equations, such as the thermal interaction term (ψ).

References

Beavers, G. S. and Joseph, D. D. 1967. Boundary conditions at a naturally permeable wall. *J. Fluid Mech.*, **30**(1), 197–207

Costa Mattos, H., Martins-Costa, M. L., Sampaio, R., and Saldanha da Gama, R. M. 1993. A thermodynamically consistent constitutive theory for a rigid solid-Stokesian fluid mixture. *Mech. Res. Comm.*, **20**(3), 243–249

Euvrard, D. 1987. Résolution Numérique des Équations aux Dérivées Partielles. Masson, Paris

Huang, P. C. and Vafai, K. 1993. Flow and heat transfer control over an external surface using a porous block array arrangement. *Int. J. Heat Mass Transfer*, **36**(1), 4019–4032

John, F. 1982. *Partial Differential Equations.* Springer-Verlag, New York

Martins-Costa, M. L., Sampaio, R., and Saldanha da Gama, R. M. 1991. An algorithm for simulating the energy transfer process in a moving solid–fluid mixture. *J. Braz. Soc. Mec. Sci.*, **13**(4), 337–359

Martins-Costa, M. L., Sampaio, R., and Saldanha da Gama, R. M. 1992. Modelling and simulation of energy transfer in a saturated flow through a porous medium. *Appl. Math. Modeling*, **16**(11), 589–597

Martins-Costa, M. L., Sampaio, R., and Saldanha da Gama, R. M. 1993. On the energy balance for continuous mixtures. *Mech. Res. Comm.*, **20**(1), 53–58

Martins-Costa, M. L., Sampaio, R., and Saldanha da Gama, R. M. 1994. Modelling and simulation of natural convection flow in a saturated porous cavity. *Meccanica – Int. J. Italian Assoc. Theoret. Appl. Mech.*, **29**, 1–13

Nield, D. A. and Bejan, A. 1992. *Convection in Porous Media.* Springer-Verlag, New York

Richardson, S. 1971. A model for the boundary condition of a porous material. Part 2. *J. Fluid Mech.*, **49**(2), 327–336

Saldanha da Gama, R. M. and Sampaio, R. 1983. Modelling for two-regions flows, one occupied by a viscous fluid and the other by a mixture. *J. Braz. Soc. Mech. Sci.*, **5**(1), 3–17

Taylor, G. I. 1971. A model for the boundary condition of a porous material. Part 1. *J. Fluid Mech.*, **49**(2), 319–326

Vafai, K. and Kim, S. M. 1990. Analysis of surface enhancement by a porous substrate. *J. Heat Transfer*, **112**, 700–706

Vafai, K. and Sozen, M. 1990. Analysis of energy and momentum transport for fluid flow through a porous bed. *J. Heat Transfer*, **112**, 690–699

Whitaker, S. 1969. Advances in theory of fluid motion in porous media. *Ind. Eng. Chem.*, **61**, 14–28

Williams, W. O. 1978. Constitutive equations for a flow of an incompressible viscous fluid through a porous medium. *Q. Appl. Math.*, **36**, 255–267